Highly Efficient Deep-Blue Emitters Based on cis and trans N-Heterocyclic Carbene Pt-II Acetylide Complexes: Synthesis, Photophysical Properties, and Mechanistic Studies

ARTICLE *in* CHEMISTRY - A EUROPEAN JOURNAL · NOVEMBER 2013

Impact Factor: 5.73 · DOI: 10.1002/chem.201302196 · Source: PubMed

3 AUTHORS, INCLUDING:

Yuzhen Zhang
University of Zurich
4 PUBLICATIONS **40** CITATIONS

SEE PROFILE

Olivier Blacque
University of Zurich
187 PUBLICATIONS **2,404** CITATIONS

SEE PROFILE

CHEMISTRY
A EUROPEAN JOURNAL

FULL PAPER

DOI: 10.1002/chem.201302196

Highly Efficient Deep-Blue Emitters Based on *cis* and *trans* N-Heterocyclic Carbene Pt^{II} Acetylide Complexes: Synthesis, Photophysical Properties, and Mechanistic Studies

Yuzhen Zhang, Olivier Blacque, and Koushik Venkatesan*[a]

Abstract: We have synthesized *cis* and *trans* N-heterocyclic carbene (NHC) platinum(II) complexes bearing σ-alkynyl ancillary ligands, namely [Pt(dbim)$_2$(C≡CR)$_2$] [DBIM = *N*,*N*′-didodecylbenzimidazoline-2-ylidene; R = C_6H_4F (**4**), C_6H_5 (**5**), $C_6H_2(OMe)_3$ (**6**), C_4H_3S (**7**), and $C_6H_4C{\equiv}CC_6H_5$ (**8**)] and [Pt(ibim)$_2$(C≡CC_6H_5)$_2$] (**9**) (ibim = *N*,*N*′-diisopropylbenzimidazoline-2-ylidene), starting from [Pt(cod)(C≡CR)$_2$] (COD = cyclooctadiene) and 2 equivalents of [dbimH]Br ([ibimH]Br for complexes **9**) in the presence of *t*BuOK and THF. Mechanistic investigations aimed at uncovering the *cis* to *trans* isomerization reaction have been performed on the representative *cis* complex **5a** [Pt(dbim)$_2$(C≡CC_6H_5)$_2$] and revealed the isomerization to progress smoothly in good yield when **5a** was treated with catalytic amounts of [Pt(cod)(C≡CR)$_2$] at 75 °C in THF or when **5a** was heated at 200 °C in the solid state under an inert atmosphere. Detailed examination of the reactions points to the possible involvement, in a catalytic fashion, of a solvent-stabilized Pt^{II} dialkyne complex in the former case and a Pt^0 NHC complex in the latter case, for the transformation of the *cis* isomer to the corresponding *trans* complex. Thermal stability and the isomerization process in the solid state have been further investigated on the basis of TGA and DSC measurements. X-ray diffraction studies have been carried out to confirm the solid-state structures of **4b**, **5a**, **5b**, and **9b**. All of the synthesized dialkyne complexes **4**–**9** exhibit phosphorescence in solution, in the solid state at room temperature (RT), and also in frozen solvent glasses at 77 K. The emission wavelengths and quantum yields have been found to be highly tunable as a function of the alkynyl ligand. In particular, the *trans* isomer of complex **9** in a spin-coated film (10 wt % in poly(methyl methacrylate), PMMA) exhibits a high phosphorescence quantum yield of 80 %, which is the highest reported for Pt^{II}-based deep-blue emitters. Experimental observations and time-dependent density functional theory (TD-DFT) calculations are strongly indicative of the emission being mainly governed by metal-perturbed interligand (^{3}IL) charge transfer.

Keywords: acetylides · isomerization · N-heterocyclic carbenes · OLEDs · phosphorescence · platinum

Introduction

Small-molecule triplet emitters and polymers based on platinum(II) complexes have received considerable attention due to their potential applications in phosphorescent organic light-emitting devices (PhOLEDs),[1] chemosensors,[2] nonlinear optical (NLO) materials,[3] photocatalysts,[4] optical limiting materials,[5] and photovoltaic devices.[6] This wide range of applications can be attributed to platinum's spin-orbit coupling constant of 4481 cm^{-1},[7] which promotes efficient intersystem crossing (ISC) from singlet to triplet excited states. When the fast ISC rates of Pt complexes are combined with a strong field ligand like an alkyne, it creates a strong interaction through pπ–dπ overlap and raises the metal-centered d–d energy states, which in turn lowers the HOMO–LUMO energy gap resulting in emissive complexes.[1i,8]

Since the time of the first report of a phosphine-ligated Pt^{II} acetylide complex, *trans*-[Pt(PEt$_3$)$_2$(C≡CPh)$_2$], by Chatt and Shaw in 1959,[9] intensive research investigations have been carried out on the photophysical properties of these complexes (Figure 1, top). Studies of the phosphorescent emission properties of small molecules,[10] oligomers,[11] dendrimers,[3c,12] and polymers[1b,13] based on phosphine Pt^{II} acetylide fragments have indicated moderate to low quantum yields with emission only in the low-energy part of the visible spectrum. The bipyridine Pt^{II} acetylide complexes first reported by Che and co-workers showed a metal–ligand charge transfer (^{3}MLCT) [5d(Pt)→π*$_{phen}$]-centered emission in fluid solution at RT.[14] Subsequently, the groups of Eisenberg,[4a,15] Schanze,[16] Castellano,[4b,8a,17] and Yam[3b,c,8b,12,18] carried out extensive investigations on similar molecular entities and in due course expanded their diversity with the use of polypyridine-type ligands [Pt(N^N^N)(C≡CR)]$^+$ [4a,4c,5b,15f,19] and [Pt(N^N^C)(C≡CR)] (Figure 1, bottom).[5a,20] The origin of the triplet emission in diimine Pt^{II} ace-

[a] Y. Zhang, Dr. O. Blacque, Dr. K. Venkatesan
Inorganic Chemistry, University of Zürich,
Winterthurerstrasse 190, 8057 Zürich (Switzerland)
Fax: (+41) 44 6356803
E-mail: venkatesan.koushik@aci.uzh.ch

Supporting information for this article is available on the WWW under http://dx.doi.org/10.1002/chem.201302196.

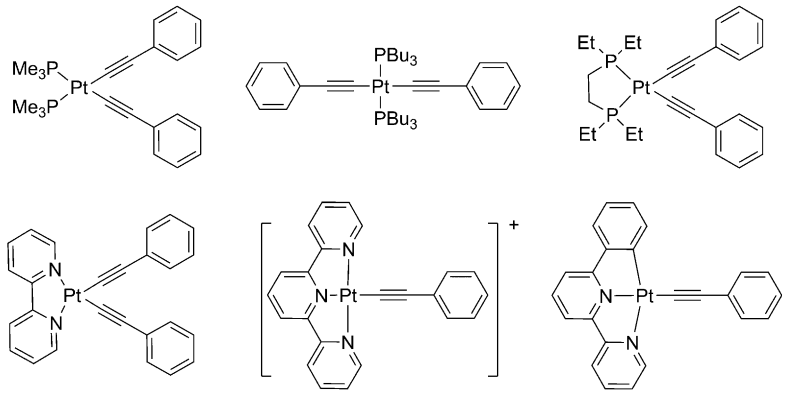

Figure 1. Platinum(II) dialkynyl complexes bearing phosphine ligands (top) and nitrogen ligands (bottom).

tylide complexes has been ascribed to a mixture of intraligand charge transfer $^3[\pi\rightarrow\pi^*(C{\equiv}CR)]$ (^{3}IL) and metal–ligand charge transfer $^3[5d(Pt)\rightarrow\pi^*(NN)]$ (^{3}MLCT) giving rise to moderate to good emission properties, albeit only at longer wavelengths.[21]

Since phosphine- and diimine-bound Pt^{II} acetylide small molecules show mostly moderate to good emission properties in the low-energy part of the visible spectrum, the development of highly emissive and stable small-molecule emitters at the high-energy end of the spectrum is highly desirable. Such systems could serve as key building blocks for the construction of new polymers and dendrimers that meet the demands of a number of applications.[16,17b,c,22] N-Heterocyclic carbene (NHC) ligands are considered as an interesting alternative to phosphine and pyridine ligands. Given that NHCs are strong σ-donors, their strong Lewis basicity would be expected to result in stronger Pt^{II}–ligand bonds, which would significantly reduce the likelihood of nonradiative deactivation of the excited states through dissociation of the ligand upon excitation.[1f,7c,23] In addition, the strong σ-donation of the NHC ligands is expected to be effective in preventing thermal access to metal-centered d–d states by pushing these to higher energies.[1h,24] The versatile coordination modes of NHCs would further allow the preparation of molecules with large conformational diversity.[13c] Exquisite control of the steric environment and electronic properties can be achieved by rational modification of the substituents on the nitrogen atoms and the NHC framework.[25] Following the report of Strassner and co-workers on dicationic blue-light-emitting tetra-NHC Pt^{II} complexes,[1d,26] we recently described the preparation and photophysical investigation of a series of neutral bis-NHC Pt^{II} acetylide and bis-NHC Pd^{II} acetylide complexes.[27] Some of the bis-NHC Pt^{II}-acetylides displayed blue emission at room temperature and the luminescent properties were found to be tunable by changing the functional group on the alkyne.[28] TD-DFT calculations revealed that the emission was dominated by intraligand charge transfer $^3[\pi\rightarrow\pi^*(C{\equiv}CR)]$ (^{3}IL), with limited participation of the metal center in the excited state. In view of the observed intriguing phosphorescence emission properties of the *cis* NHC Pt^{II} dialkyne complexes in solution and the solid state, the *trans* NHC Pt^{II} dialkyne complexes were expected to be suitable candidates as novel building blocks for the preparation of linear organometallic oligomers, dendrimers, macrocycles, and polymers. NHC ligands bearing dodecyl chains have been used to enhance the solubility of the final complexes.

In this context, we report herein detailed investigations on the synthesis, solid-state structures, and luminescent properties of new *trans* bis-NHC Pt^{II} bisacetylide complexes. Different reaction conditions have been employed to prepare the *trans* complexes in high yields, and studies have been carried out aimed at elucidating the mechanism underpinning their formation. Since the electronic properties of the alkyne ligands were expected to strongly influence the luminescent properties, complexes bearing different alkyne ligands were targeted, and experimental and theoretical investigations were carried out to analyze the nature of the excited states. The remarkable quantum yields of the *trans* complexes of **4** and **5** in the solid state are the highest reported for deep-blue emitters. The readily tunable emission properties hold great promise for the potential use of this fragment in the construction of light-emitting macromolecules for varied applications.

Results and Discussion

Synthesis and characterization: Transition metal alkynyl complexes are mostly synthesized by well-known transmetallation procedures involving copper acetylides, alkynyl stannanes, or lithium acetylides starting from the readily accessible metal halide complexes. However, previous studies have shown that *trans* $[Pt(dbim)_2Br_2]$[29] (DBIM = *N*,*N*′-diisopropylbenzimidazoline-2-ylidene), particularly bearing nonsterically demanding substituents at the nitrogen atoms, can only be generated in a dismal yield (3%), and hence this approach was discarded. $[Pt(cod)(C{\equiv}CR)_2]$ (cod = cyclooctadiene) was considered as a suitable precursor, since the labile COD ligand was expected to be readily displaced in the presence of the NHC ligand due to the strong *trans* effect of the alkynyl ligand. Based on an earlier literature protocol, the precursor complexes of the type $[Pt(cod)(C{\equiv}CR)_2]$ (R = C_6H_4F (**1**), C_6H_5 (reported),[30a] $C_6H_2(OCH_3)_3$ (**2**), 2-thienyl (**3**), and $C_6H_4C{\equiv}CC_6H_5$ (reported)[30b]) were obtained in good to moderate yields by treating $[Pt(cod)Cl_2]$ with the corresponding sodium acetylides in ethanol.[31] Subsequent treatment of $[Pt(cod)(C{\equiv}CC_6H_5)_2]$ with 2 equivalents of DBIM in THF at 75 °C resulted in a mixture of two

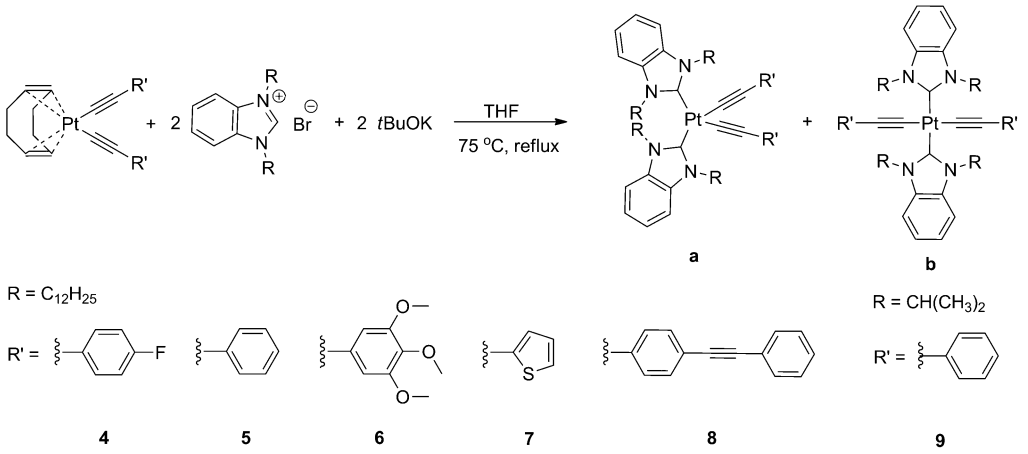

Scheme 1.

complexes. The ^{1}H NMR spectrum of the mixture featured three multiplets at $\delta = 4.89$, 4.86, and 4.38 ppm, characteristic resonances of the -CH_2 protons bound to the α-C connected to the benzimidazole nitrogen ($NCH_2C_{11}H_{23}$). ESI-MS analysis of the mixture gave a peak at m/z 1330.0 $[M+Na]^+$. Based on detailed NMR studies, the multiplets at $\delta = 4.89$ and 4.38 ppm were assigned to the *cis* isomer **5a** and that at $\delta = 4.86$ ppm to the *trans* isomer **5b** (Figure 2).

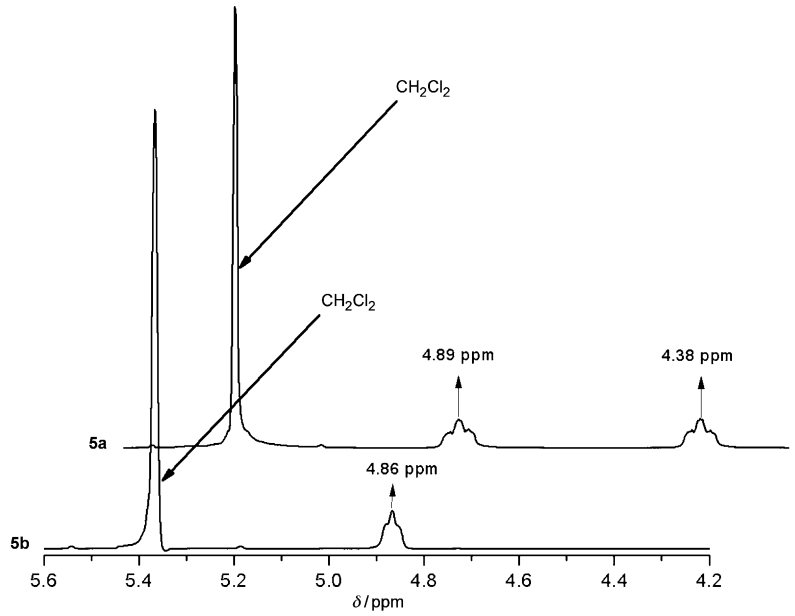

Figure 2. ^{1}H NMR spectra of *cis* complex **5a** and *trans* complex **5b**.

The two products were obtained in yields of 27 and 24%, respectively, after separation by column chromatography on silica gel. Single-crystal X-ray diffraction studies further confirmed the structures of **5a** and **5b**. Analogously, various *cis* and *trans* complexes of the type $[Pt(dbim)_2(C{\equiv}CR)_2]$ (R = C_6H_4F (**4a**,**b**); C_6H_5 (**5a**,**b**); $C_6H_2(OCH_3)_3$ (**6a**,**b**); 2-thienyl (**7a**,**b**); $C_6H_4C{\equiv}CC_6H_5$ (**8a**,**b**)) and $[Pt(ibim)_2(C{\equiv}CR)_2]$ (R = C_6H_5 (**9a**,**b**)) were synthesized (Scheme 1). The isolated yields were between 9 and 42% for the *cis* isomers and between 4 and 27% for the *trans* isomers, depending on the alkyne substituents. All of the *cis* and *trans* complexes were characterized by ^{1}H NMR, ^{13}C NMR, and IR spectroscopy, as well as ESI-MS. The structure of **4b** was also confirmed by a single-crystal X-ray diffraction study. In order to improve the yield of the highly desired *trans* product and to account for the observation of both *cis* and *trans* product during the reaction, further investigations were carried out. When the reaction was performed at room temperature by using 3.0 equivalents of the NHC ligand instead of the original 2.0 equivalents, a near-quantitative yield of **5a** was obtained with only a trace of the *trans* isomer. Significant improvements in the yields (47–90%) of the respective *cis* isomers were accomplished when 3.0 equivalents of the NHC were used in the reaction.

Single-crystal X-ray diffraction analysis: Single crystals suitable for X-ray diffraction were grown by slow evaporation of the solvent from a concentrated solution of the compound in a mixture of MeOH and CH_2Cl_2. The molecular structures of complexes **4b**, **5a**, **5b**, and **9b** are shown in Figure 3. Crystallographic parameters are summarized in Table S1 in the Supporting Information and selected bond lengths and angles are listed in Table 1. The four complexes exhibit distorted square-planar coordination geometries about the Pt^{II} core. The $Pt{-}C_{carb}$ distances in the complexes range from

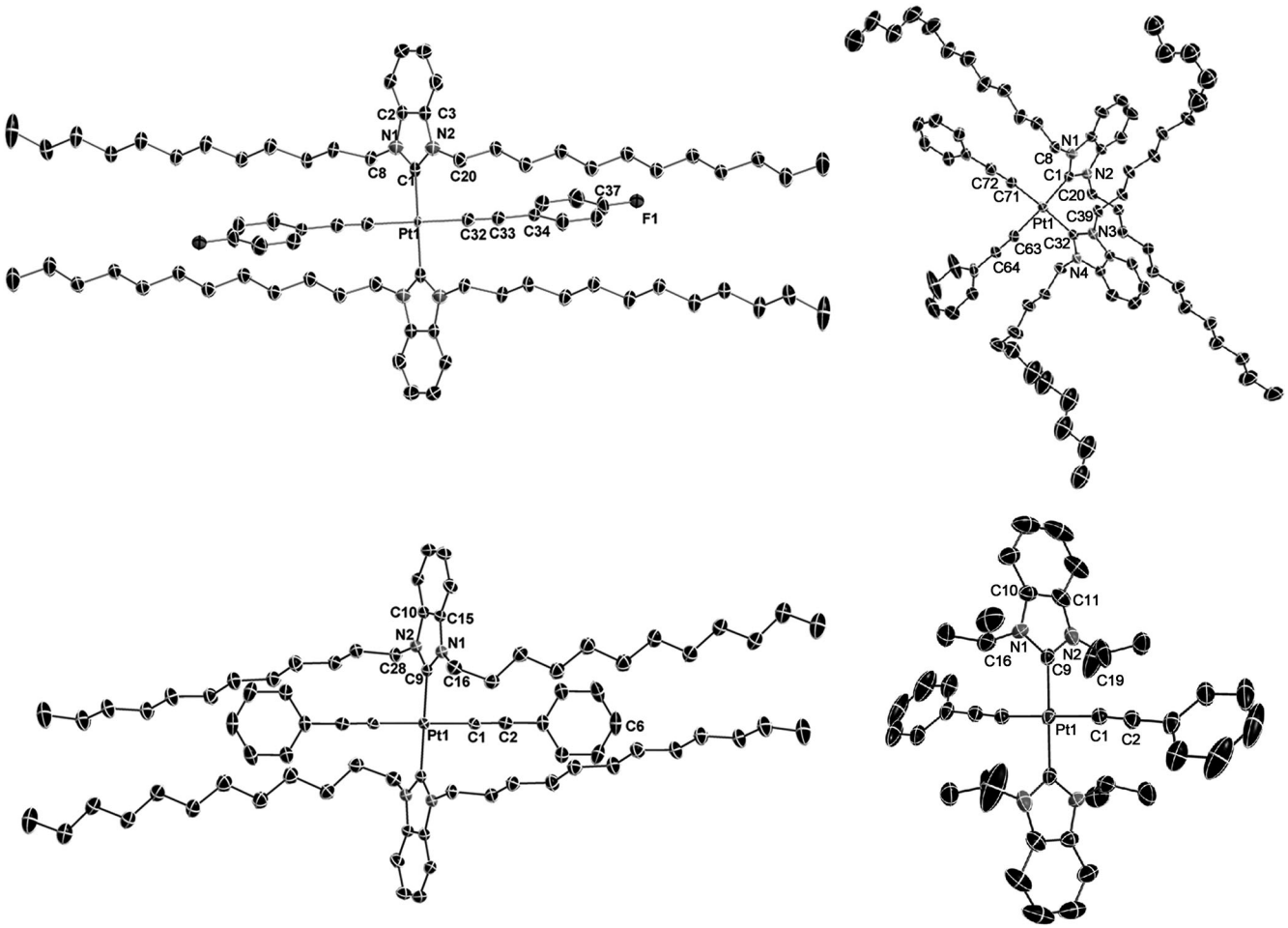

Figure 3. Molecular structures of **4b**, **5a**, **5b**, and **9b** showing selected atomic numbering. Ellipsoids are set at the 50% probability level. Hydrogen atoms and solvent molecules are omitted for clarity

2.0168(18) to 2.029(3) Å and the Pt–C_{alk} distances from 1.996(3) to 2.0092(18) Å. The Pt–C_{carb} distances in the current complexes are longer than those in previously reported analogous structures, which may be due to the *trans* influence of the strongly electron-donating acetylene ligands.[29,32] The Pt–C_{alk} distances are shorter than those in reported [Pt(phosphine)$_2$(C≡CR)$_2$] complexes,[33] but 0.04 Å longer than those in [Pt(bipyridine)(C≡CR)$_2$] complexes.[15a,21] The Pt–C_{carb} distance in **5a** is 0.01 Å longer than that in **5b**, but the reverse is true for the Pt–C_{alk} distances. The shortest Pt···Pt distance in these structures was found to be 8.6169(2) Å, and hence any intermolecular Pt···Pt interaction in the solid state can be ruled out.

UV/Vis absorption and emission: The UV/Vis absorption spectra of complexes **4**–**9** in solution at 298 K are shown in Figure 4 and Figure S1 in the Supporting Information. All ten complexes exhibit similar spectra, with an intense absorption band at 284–300 nm and an additional shoulder band (low-energy absorption bands) at 305–358 nm. The molar absorption coefficients (ε) for the intense absorption bands are in the range 2.0×10^4 to $6.0\times10^4\,M^{-1}cm^{-1}$, and are thus comparable to those of reported [Pt(diimine)(C≡CR)$_2$] complexes. In comparison with the spectra of our previously reported bidentate NHC Pt^{II} acetylide complexes, the low-energy absorption bands are hypsochromically shifted by approximately 40 nm and overlap with the high-energy bands. Varying the solvent in further UV/Vis studies on these complexes showed no significant shifts in the absorption wavelengths.

Based on the spectroscopic studies and the DFT and TD-DFT calculations, the low-energy absorption bands in these ten complexes are assigned to a mixture of metal-perturbed ligand-to-ligand ^{1}LLCT ($\pi_{alk}\rightarrow\pi^*_{carb}$) and metal-to-ligand ^{1}MLCT (5d(Pt)$\rightarrow\pi^*_{carb}$) transitions.[15a,21] The high-energy absorption bands that display the characteristic $\pi\rightarrow\pi^*$ transition are assigned to metal-perturbed intraligand ^{1}LLCT ($\pi_{alk}\rightarrow\pi^*_{alk}$) transitions.[16,18b,20a] There are no significant differences in the patterns of the absorption bands and absorption maxima for complexes **4**–**7** and **9**. However, in the case of complexes **8a** and **8b** bearing the conjugated ligand C≡CC_6H_4C≡CC_6H_5, the absorption bands are further redshifted to 343 and 353 nm, respectively. The observed redshifts in the absorptions of **8a** and **8b** in comparison to those of the

Table 1. Selected bond lengths [Å] and angles [°] of complexes **4b**, **5a**, **5b**, and **9b**.

	Distance [Å]	Angle [°]	
Complex **4b**			
C(1)−Pt(1)	2.020(2)	C(1)-Pt(1)-C(32)	88.85(8)
C(32)−Pt(1)	2.0092(18)	C(1)-Pt(1)-C(32)^{i}	91.15(8)
Complex **5a**			
C(1)−Pt(1)	2.026(3)	C(63)-Pt(1)-C(71)	84.14(13)
C(32)−Pt(1)	2.029(3)	C(71)-Pt(1)-C(1)	91.42(12)
C(63)−Pt(1)	1.996(3)	C(63)-Pt(1)-C(32)	92.16(12)
C(71)−Pt(1)	2.006(3)	C(1)-Pt(1)-C(32)	92.37(11)
Complex **5b**			
C(1)−Pt(1)	2.0043(19)	C(1)-Pt(1)-C(9)	88.60(7)
C(9)−Pt(1)	2.0168(18)	C(1)-Pt(1)-C(9)^{i}	91.40(7)
Complex **9b**			
C(1)−Pt(1)	2.008(2)	C(1)-Pt(1)-C(9)	93.03(8)
C(9)−Pt(1)	2.027(2)	C(8)-Pt(1)-C(1)	86.97(8)

$[i] -x, -y, -z$.

other eight complexes reflect the smaller HOMO–LUMO gaps arising from the increased conjugation of the alkyne ligand. Comparison of the UV/Vis absorption bands between the isomers revealed those of the *trans* isomers to be slightly bathochromically shifted with lower molar absorption coefficients than those of the corresponding *cis* isomers.

All of the synthesized dialkyne complexes were found to be emissive both in solution and the solid state. The emission spectra of the complexes recorded in CH_2Cl_2 featured bands in the range 431–530 nm (Table 2). The large Stokes shifts ($\approx$150 nm), along with emission lifetimes of the order of microseconds and rapid quenching of the emission in air, are highly indicative of emission from a triplet manifold. The emission wavelengths of the *cis* complexes **4a**–**6a** are bathochromically shifted with increasing electron-donating character ($F < H < (OMe)_3$) of the substituents on the alkynes. A similar trend was seen for the *trans* isomers **4b**–**6b**. All of the *trans* isomers show a 3–6 nm redshift in their emission maxima compared to the corresponding *cis* isomers. This can be attributed to the efficient charge delocalization in the highly symmetrical *trans* isomer, resulting in a decrease in the HOMO–LUMO gap. Complexes **7a** and **7b** exhibit broad bands along with a strong vibronic progression due to the thienyl group. Their emission maxima are also bathochromically shifted by about 70 nm compared to those of complexes **6a** and **6b**. In accordance with the different electron donicities and electron delocalization of the alkynyl substituents, the emission maxima of complexes **8a** and **8b** bearing $C{\equiv}CC_6H_4C{\equiv}CC_6H_5$ are significantly redshift-

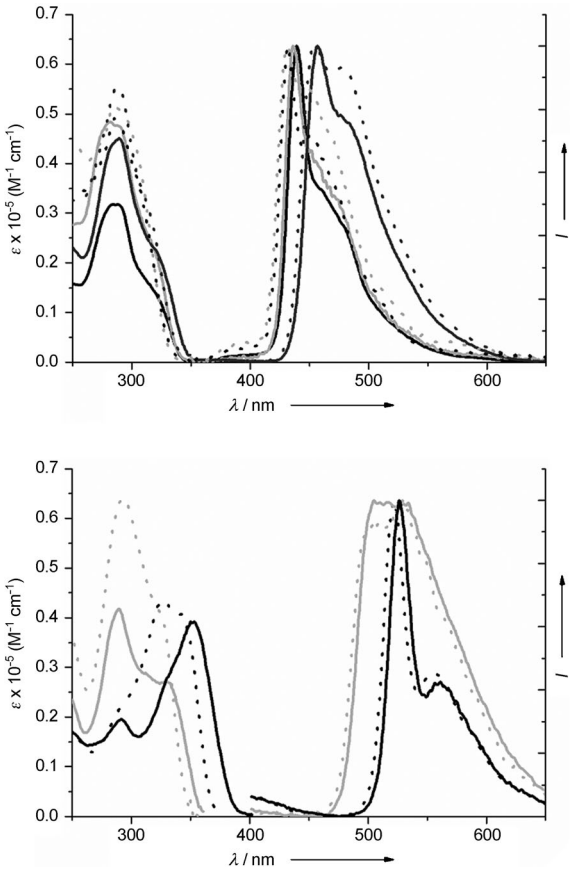

Figure 4. Top) Electronic absorption and normalized emission spectra of **4a** (light-gray dotted line), **4b** (light-gray solid line), **5a** (black dotted line), **5b** (black solid line), **6a** (dark-gray dotted line), **6b** (dark-gray solid line) in CH_2Cl_2 at RT. Bottom) Electronic absorption and normalized emission spectra of **7a** (light-gray dotted line), **7b** (light-gray solid line), **8a** (black dotted line), and **8b** (black solid line) in CH_2Cl_2 at RT.

Table 2. Photophysical properties of complexes **4a**–**9a** and **4b**–**9b**.

	Room temperature solution (CH_2Cl_2)								77 K Glass	10 wt % PMMA Film	
	Absorption λ_{max} [nm] (ε_{max}/[$dm^3 mol^{-1} cm^{-1}$])	Emission λ_{max} [nm] Solution	Solid state	τ [μs]	$\phi_{em} \times 10^{-2}$ CH_2Cl_2	Solid	k_r [$\times 10^3$ s^{-1}]	k_{nr} [$\times 10^5 s^{-1}$]	(2-MeTHF) Emission λ_{max} [nm]	Emission λ_{max} [nm]	$\phi_{em} \times 10^{-2}$
4a	284 (51634), 293 (50335)	431, 462 sh	432, 450 sh, 472 sh	0.22	0.4	7.1	19	45	422, 440 sh	429, 449	65.1
5a	285 (49082), 300 (39978)	432, 465 sh	430, 450 sh, 475 sh	0.24	0.9	1.6	36	41	425, 447 sh	431, 449	60.8
6a	289 (55406), 310 (33877)	454, 478 sh	454, 471 sh, 505 sh	3.48	1.2	0.2	3.4	2.8	442, 475 sh	454, 484	7.5
7a	293 (64198), 322 (41740)	529, 533 sh	496, 511, 531, 550	7.90	0.4	0.5	0.4	1.3	488, 503	506, 531	5.0
8a	327 (43462), 343 (40726)	522, 554 sh	526, 558, 573 sh	6.80	0.4	3.4	0.5	1.4	516, 548 sh	523, 558	5.2
9a	285 (47827), 302 (34208)	432, 465 sh	432, 450 sh, 460 sh	0.10	0.1	0.8	10	9.9	420, 448 sh	431, 450	53.6
4b	281 (48381), 311 (26955)	436, 471 sh	416, 431 sh, 457 sh	0.37	2.6	44.5	70	26	426, 445 sh	434, 457 sh	52.6
5b	288 (31751), 315 (15709)	439, 461 sh	443, 465 sh, 487 sh	3.58	1.0	46.6	2.7	2.8	430, 451 sh	440, 460 sh	44.7
6b	289 (45128), 318 (23190)	457, 498 sh	463, 481 sh, 523 sh	2.52	1.9	0.2	7.5	3.9	440, 473 sh	453, 484	7.7
7b	289 (41746), 333 (26741)	505 sh, 534	502, 516, 538, 556	2.41	0.3	0.4	1.4	4.1	488, 504	511, 535	1.5
8b	291 (19531), 353 (39222)	527, 561	529, 561, 576 sh	5.30	0.8	5.7	1.4	1.8	522, 555	525, 563	6.9
9b	283 (34110), 310 (18219)	439, 455 sh	438, 451 sh	1.11	0.9	4.1	8.1	8.9	423, 450 sh	436, 456	80.0

ed to 522 and 527 nm, respectively. The triplet emissions are assigned to the metal-perturbed ligand-to-ligand ($\pi_{alk} \rightarrow \pi^*_{alk}$) transition. An increase in ligand donicity raises the alkynyl-based HOMO energy level, thereby decreasing the energy gap between the HOMO and LUMO, which in turn results in a bathochromic shift of the emission. The solution quantum yields of complexes **4**–**9** were found to lie in the range 1.0×10^{-3} to 2.6×10^{-2} by using quinine sulfate as a reference ($\phi_{em}=0.55$). These are comparable to those of known [Pt(diimine)(C≡CR)$_2$] complexes and our previously reported chelating NHC Pt acetylide complexes.

In a rigidified glass medium (2-methyltetrahydrofuran, 2-MeTHF) at 77 K, the spectra of **4**–**9** are well-resolved, as shown in Figures S2 and S3 in the Supporting Information. The emission maxima of the complexes are in the wavelength range 422–522 nm, shifted by 5–58 nm compared with those at RT. Unlike the broad and unsymmetrical emission profiles at room temperature, the spectra at 77 K exhibit a rigidochromic shift and resolvable vibronic components of the emission. The vibrational progressional spacings of **7a** are 650 and 1450 cm^{-1}, which can be assigned to the characteristic skeletal vibration of the thienyl ring, and 2041 cm^{-1}, which can be assigned to the $\tilde{\nu}_{(C\equiv C)}$ stretching vibration of (Figure S4 in the Supporting Information). Complex **7b** was found to exhibit similar behavior to that of **7a**. The vibrational progressional spacings of complex **8b** are 1106, 1613, and 2092 cm^{-1}, which can be assigned to the C–N stretching vibration, the skeletal vibration of the phenyl ring, and the $\tilde{\nu}_{(C\equiv C)}$ stretching vibration, respectively (Figure S4 in the Supporting Information). Complex **8a** exhibits a similar behavior. The rest of the complexes display features like those of **4b** (Figure S5 in the Supporting Information), comprising two vibrational progressional spacings of 1100 cm^{-1} (C–N stretching vibration of benzimidazole) and 2100 cm^{-1} ($\tilde{\nu}_{(C\equiv C)}$ stretching vibration). These vibronic emission peaks further support the involvement of the alkynyl ligand in the triplet emission. At 77 K, the emission maxima of the *trans* isomers show moderate redshifts with respect to those of the corresponding *cis* isomers, although for complex **6b** the redshift is only 2 nm relative to the maximum for **6a**. This difference is also reflected in the oxidation potentials of the complexes derived from the CV measurements of the *cis* and *trans* complexes (see below). All of the synthesized complexes **4**–**9** show emission in the solid state. The absolute quantum yields of all of the *cis* and *trans* complexes in pure crystalline form were measured. Interestingly, the maxima of the triplet emissions of all the complexes appear at different wavelengths in different media due to the effects of the solvent environment and molecular aggregation (Figures S6–S8 in the Supporting Information). These influences also extend to the luminescent efficiencies of the complexes. The quantum yields of most of the complexes in fluid solution were found to lie in a low range from 0.1 to 2.6%, but increased to 47% in the case of complex **5b**. Moreover, when the complexes were dispersed at 10 wt% in poly(methyl methacrylate) (PMMA) films, their quantum yields were found to be significantly enhanced, to 80% in the case of complex **9b**. The absorption and emission spectra of complexes **9a** and **9b** were the same as those of complexes **5a** and **5b**. However, the quantum yields of **5b** and **9b** at 10 wt% in PMMA differed significantly.

Based on the above results, we can conclude that increased molecular rigidity and weaker intermolecular interactions in the solid state lead to a significant enhancement in quantum efficiency in molecules of this type. The development of blue-emitting Pt^{II} complexes has been notoriously difficult, and only recently have quantum yields of 90 and 86% with $\lambda_{em}=464$ nm been reported by the groups of Strassner[1d] and Wang[1f] by using cyclometalated ligands. To the best of our knowledge, the emission quantum yield of 80% for **9b** with $\lambda_{em}=436$ nm is the highest reported for a deep-blue emitter in this range. This work provides further impetus to the design of highly emissive deep-blue emitters devoid of a cyclometalating ligand.

Electrochemistry: Cyclic voltammograms of complexes **4**–**8** were measured in DMF by using [nBu$_4$N][PF$_6$] (0.1 M) as supporting electrolyte. The electrochemical data are listed in Table 3. There is only one irreversible oxidation wave for each complex and no observable reduction wave on scanning up to −2.57 V (Figure S9 in the Supporting Information). This behavior is consistent with the stronger σ-donating nature of the NHC ligand and quite closely resembles that of analogous [Pt(phosphine)$_2$(C≡CR)$_2$] complexes. However, it differs from that of [Pt(diimine)(C≡CR)$_2$] complexes, which show one or more reversible reduction waves associated with the diimine ligand. For complexes **4**, **5**, and **6**, the oxidation potential decreases with increasing donor ability of the alkynyl functional group (F < H < (OMe)$_3$). Comparing the oxidation potentials of the respective pairs of *cis* and *trans* isomers, that of the *cis* isomer is about 50–110 mV higher than that of the *trans* isomer, except in the case of compounds **6a** and **6b**. This abnormal behavior of **6a** and **6b** is consistent with the emission maxima observed at 77 K, with **6b** emitting at a higher energy than **6a**. The oxidation waves observed for all of the complexes are tentatively assigned to oxidation of the alkynyl ligand rather than a Pt^{II}/Pt^{III} process given the low oxidation potential (< +1.0 V) and since the HOMO (93%) is mainly located on the C≡CR π orbital, according to DFT calculations.

Table 3. Electrochemical potentials for **4a**–**9a** and **4b**–**9b**.[a]

Complex	E_{ox} [V]	Complex	E_{ox} [V]
4a	+0.86	**4b**	+0.79
5a	+0.84	**5b**	+0.77
6a	+0.58	**6b**	+0.66
7a	+0.86	**7b**	+0.75
8a	+0.94	**8b**	+0.83
9a	+0.85	**9b**	+0.78

[a] Scan rate = 100 mV s^{-1} in 0.1 M [nBu$_4$N][PF$_6$] (Au electrode; E vs Fc$^+$/Fc; 20 °C; DMF).

DFT calculations: In order to study the luminescent properties of our *cis* and *trans* N-heterocyclic carbene Pt^{II} acetylide complexes, we performed DFT and TD-DFT calculations on **5a** and **5b** with the Gaussian 03 program package.[34] The hybrid functional PBE1PBE (also known as PBE0)[35] in conjunction with the Stuttgart/Dresden effective core potentials (SDD) basis set[36] for the Pt center, augmented with one f-polarization function (exponent = 0.993), and the standard 6-31+G(d) basis set[37] for the remaining atoms were applied for all calculations. Full geometry optimizations without symmetry constraints, but with a C_2H_5 model instead of the long $C_{12}H_{25}$ chain of the carbene ligands in **5a** and **5b**, were carried out in the gas phase for the singlet ground states (S_0) and the lowest triplet states (T_1). The optimized geometries were confirmed to be potential energy minima by vibrational frequency calculations at the same level of theory, as no imaginary frequency was found. The first ten singlet–singlet and singlet–triplet transition energies were computed for the optimized S_0 geometries, by using the time-dependent DFT (TD-DFT) methodology. Solvent effects were taken into account by using the conductor-like polarizable continuum model (CPCM) with dichloromethane (absorption/emission) or toluene (mechanistic study) as solvent for single-point calculations on all of the optimized gas-phase geometries.

The experimental UV/Vis absorption spectra of complexes **5a** and **5b** in solution (dichloromethane) at 298 K exhibit similar absorption patterns with intense absorption bands at 285 and 288 nm and shoulder absorption bands at 300 and 315 nm, respectively. Based on the spectroscopic studies, the low-energy absorption bands in these complexes are assigned to a mixture of metal-perturbed ligand-to-ligand ^{1}LLCT ($\pi_{alk}\rightarrow\pi^*_{carb}$) and metal-to-ligand ^{1}MLCT ($5d(Pt)\rightarrow\pi^*_{carb}$) transitions. The high-energy absorption bands, which show the characteristics of $\pi\rightarrow\pi^*$ transitions, are assigned to metal-perturbed intraligand ^{1}ILCT ($\pi_{alk}\rightarrow\pi^*_{alk}$) transitions. TD-DFT calculations carried out on the ground-state structures of **5a** and **5b** confirmed the experimental analyses. In the ground-state geometry, the lowest significant singlet excited states S_1, S_3, and S_8 ($f>0.05$) of **5b** are calculated to give rise to discrete HOMO→LUMO, HOMO→LUMO+1, and HOMO−1→LUMO+3 excitations at 327 ($f=0.238$), 301 ($f=0.860$), and 278 nm ($f=0.597$), respectively (Table S2 in the Supporting Information). The LUMO is of π^* character with the electron density delocalized over both carbene ligands (82%) in an out-of-phase combination with a Pt 5d orbital (11%). On the contrary, the HOMO is located mainly on one alkyne ligand (77%) and on the metal center (23%) and has no contribution from the carbene ligands (Figure 5 and Table S3 in the Supporting Information). The HOMO−1 is almost degenerate with the HOMO, showing a main contribution from the other alkyne ligand. The participation of the metal is slightly greater in the HOMO than in the HOMO−1 (23 vs. 16%), which destabilizes the former orbital and accounts for the energy gap between these two orbitals ($\Delta E_{H-1/H}=0.17$ eV). The electron densities in the LUMO+1 and LUMO+3 are located mainly on the same alkyne ligand as the HOMO and HOMO−1, respectively. We can therefore surmise that the intense absorption band observed experimentally at 288 nm arises from overlap of the TD-DFT-calculated $S_0\rightarrow S_3$ and $S_0\rightarrow S_8$ singlet–singlet transitions and shows, in agree-

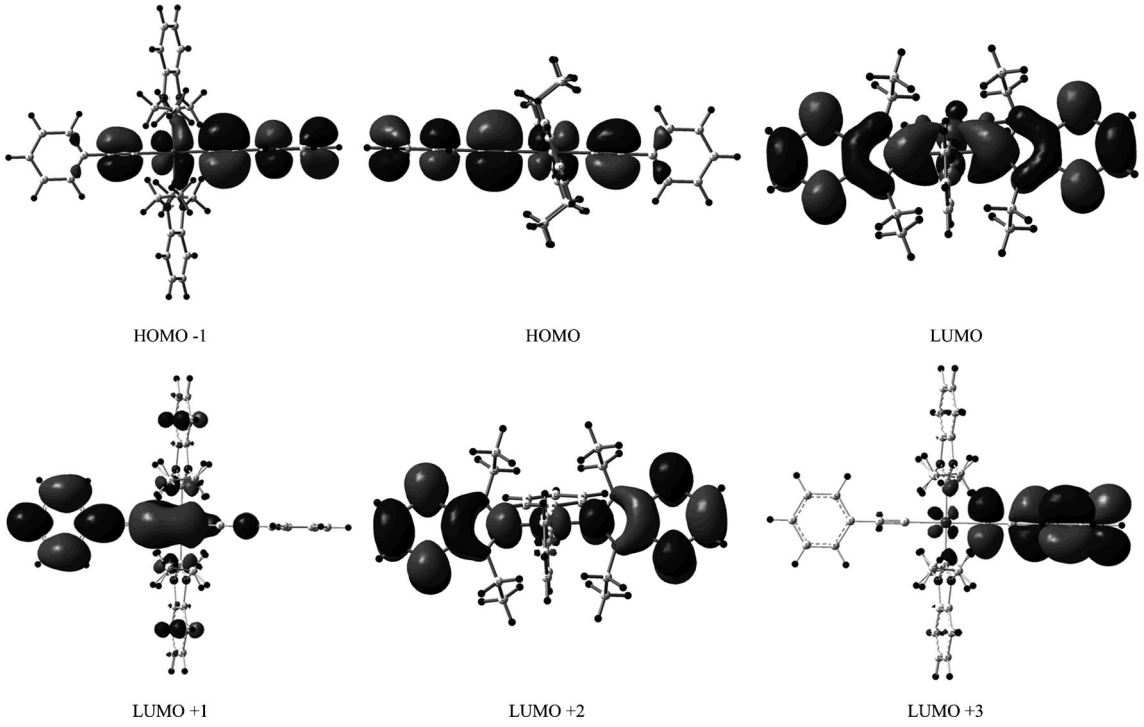

Figure 5. Spatial plots of selected frontier orbitals of the DFT-optimized ground state of **5b**.

ment with the experimental indications, intraligand ^{1}ILCT ($\pi_{alk}\rightarrow\pi^*_{alk}$) charge-transfer character. The low-energy absorption band, observed as a shoulder in the experimental UV/Vis spectrum, corresponds to the single HOMO→LUMO excitation assigned to an admixture of ligand-to-ligand ^{1}LLCT ($\pi_{alk}\rightarrow\pi^*_{carb}$) and metal-to-ligand ^{1}MLCT ($5d\rightarrow\pi^*_{carb}$) characteristics.

For complex **5a**, the assignment of the experimental bands and lowest-energy transitions is not as trivial as in the case of **5b**. Indeed, TD-DFT calculations showed only three singlet–singlet transitions (among the ten lowest transitions calculated) with an oscillator strength $f>0.1$ for **5b**, whereas no fewer than six transitions with $f>0.2$ were computed for **5a**. Furthermore, one transition exhibits a large oscillator strength of 0.860 for **5b**, whereas all transitions of **5a** are more or less equivalent ($f=0.204$–0.380). In the ground-state geometry, the lowest significant singlet excited states S_1 and S_2 of **5a** are calculated to give rise to HOMO→LUMO and HOMO−1→LUMO excitations at 320 ($f=0.357$) and 307 nm ($f=0.380$), respectively. In the HOMO and HOMO−1, the electron density is mainly located on both alkyne ligands (81–85%) in an out-of-phase combination with a Pt 5d orbital (15–16%). The bonding (HOMO−1) and antibonding orbitals (HOMO) of **5a** and **5b** differ in the through-space interactions between the alkyne ligands (Figure 6). The main difference compared to **5b** is that the unoccupied orbital involved in the one-electron excitation, here the LUMO, is delocalized over the whole molecule: 46% on the carbene ligands, 40% on the alkyne ligands, and 14% on the metal center. Considering that the low-energy absorption band (observed as a shoulder in the UV/Vis spectrum) is produced by the overlap of these two transitions, this energy absorption predominately arises from excited states with a ligand-to-ligand ^{1}LLCT ($\pi_{alk}\rightarrow\pi^*_{carb}$) charge transfer, as in **5b**, but with sizable amounts of metal-to-ligand ^{1}MLCT ($5d\rightarrow\pi^*_{carb}$) and intraligand ^{1}ILCT ($\pi_{alk}\rightarrow\pi^*_{alk}$) character. At higher energies, four transitions overlap to produce the intense experimental band at 285 nm ($S_0\rightarrow S_5$, 292 nm, $f=0.204$; $S_0\rightarrow S_8$, 282 nm, $f=0.298$; $S_0\rightarrow S_9$, 278 nm, $f=0.326$; $S_0\rightarrow S_{10}$, 277 nm, $f=0.292$). All frontier orbitals in the range HOMO−2 to LUMO+3 play a role in the single excitations of these four transitions, leading to an unclear assignment of the band.

The lowest singlet–triplet vertical excitation (T_1–S_0) energies obtained by TD-DFT calculations on the ground-state structures of **5a** and **5b** are 431 and 437 nm, which are consistent with the experimental emissions at 425 and 430 nm, respectively. The transitions responsible for the emission bands comprise the HOMO↔LUMO ($a_i=0.438$) and HOMO−1↔LUMO+3 ($a_i=0.417$) single excitations for **5a**, and the HOMO↔LUMO+1 excitation for **5b**. As already mentioned, the HOMO and HOMO−1 are mainly located on both alkyne ligands in an out-of-phase combination with a Pt 5d orbital, whereas the LUMO is delocalized over the whole molecule. The LUMO+3 is 98% localized on both alkyne ligands. The promotion of one electron to an unoccupied orbital leads to a singlet excited state, and then a spin-orbit interaction between excited states operates to induce S→T intersystem crossing to form the corresponding triplet excited state. Geometry relaxation of the latter leads to the lowest-energy triplet state, the optimized structure of which can be determined by DFT calculations. Careful analysis of the molecular orbital diagrams of the optimized triplet states of **5a** and **5b** revealed that the highest singly occupied molecular orbitals (SOMOs) are located almost exclusively on the alkyne ligands (Table S2 in the Supporting Informa-

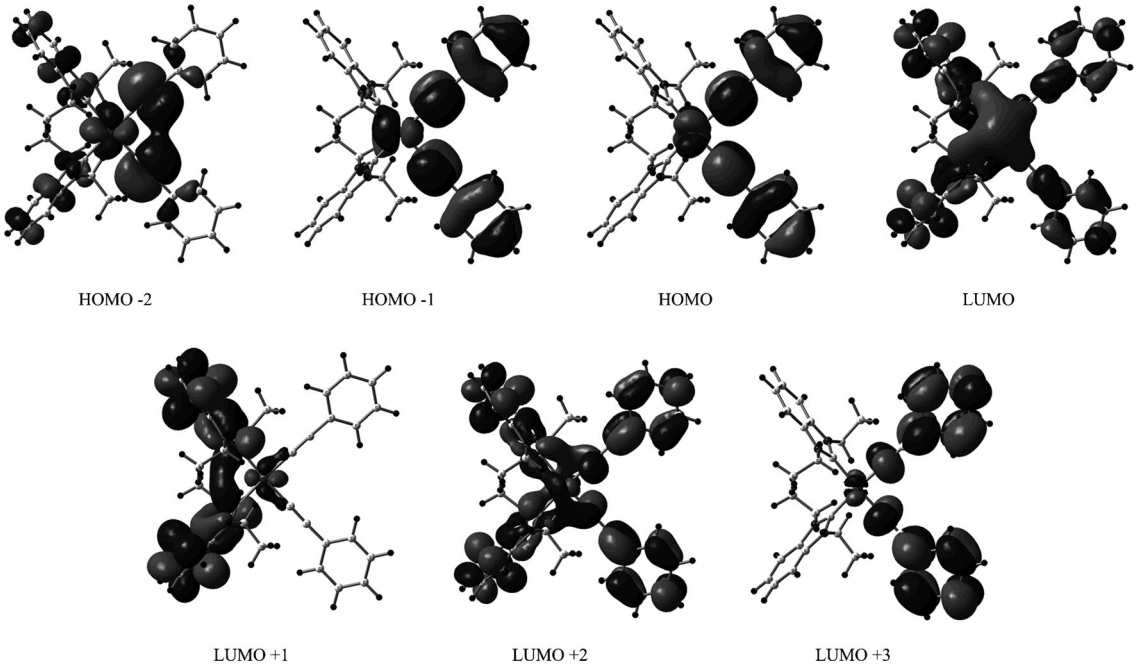

Figure 6. Spatial plots of selected frontier orbitals of the DFT-optimized ground state of **5a**.

tion). The highest SOMO, from which the emission is produced, is localized at 95 (**5a**) and 93% (**5b**) on one alkyne ligand and 5 (**5a**) and 7% (**5b**) on the metal center, whereas the second highest SOMO, called SOMO−1, to which the excited electron should return, is localized at 85% on the other alkyne ligand and 13% on the metal center (both **5a** and **5b**). The spin density surfaces of **5a** and **5b**, which take into account the electron density on all singly occupied orbitals and not only the SOMOs, visually identify the emission from a transition with mainly intraligand ^{3}ILCT ($\pi^*_{alk}\rightarrow\pi_{alk}$) character and minor ligand-to-ligand ^{3}LLCT character (Figure S10 in the Supporting Information).

Mechanistic investigations: Investigations of the *cis* to *trans* isomerization of square-planar Pt^{II} complexes have been carried out since the 1950s.[9,38,39] The mechanisms of isomerization in this class of complexes can be divided into two major categories. The first involves consecutive displacement, consisting of ligand dissociation resulting in the formation of a three-coordinate intermediate, whereas the second involves pseudorotation, consisting of an intramolecular rearrangement accompanied by formation of a five-coordinate intermediate.[39d,40] In spite of extensive mechanistic studies on this class of complexes, mechanisms for the photochemically and thermally induced isomerizations still remain elusive.[39e]

In order to determine the optimal conditions for obtaining the *trans* complexes in high yields, we set out to elucidate the possible intermediates involved in the *cis* to *trans* isomerization process. The dependence of product formation on stoichiometry was first examined by varying the ratio of NHC and precursor in [D_8]THF at 75°C (Figure S11 in the Supporting Information). The results revealed initial formation of the *cis* isomer and the *cis* isomer was found to scale up with increase in the stoichiometry of the NHC ligand. When the reaction was closely monitored by ^{1}H NMR spectroscopy with a 1:2 stoichiometry of precursor to NHC ligand, resonances attributable to the *cis* isomer were first detected, along with signals of both COD bound to the Pt^{II} center in a monodentate fashion and unbound COD.[41] The proton resonances of the bound monodentate COD appeared further downfield than those of the free COD.

Additional 1D-TOCSY NMR experiments further confirmed the presence of the intermediate (Figure S12 in the Supporting Information). Based on this observation, a plausible mechanism involving stepwise substitution with the two NHC ligands is proposed in Scheme 2. The *trans* isomer was confirmed to be the thermodynamically more stable product, since resonances in the ^{1}H NMR spectrum corresponding to this isomer started to appear when the reaction mixture containing the *cis* complex was further heated to 75°C.

Precursor-catalyzed isomerization: After carrying out several reactions in different reactant combinations,[42] we found a notable *cis* to *trans* conversion only when **4a** was treated with a stoichiometric amount of [Pt(cod)(C≡CC_6H_5)$_2$] in THF at 75°C for 24 h. The yield of **4b** was 71% (see the Supporting Information). This finding is consistent with the formation of a small amount of the *trans* isomer when only 2.0 equivalents of the NHC ligand is used, whereas little or none of the *trans* isomer was observed when using 3.0 equivalents of the NHC ligand. The conversion of **5a** to **5b** in a similar yield of 64% was accomplished by treating only 10% of the precursor complex [Pt(cod)(C≡CC_6H_5)$_2$], but the reaction proceeded very slowly (see the Supporting Information). This can be rationalized by the hypothesis that the initially formed *cis* isomer reacts with an intermediate COD-free solvent-stabilized Pt^{II} complex [(S)$_2$Pt(C≡CC_6H_5)$_2$] (S = THF).[43] The interaction between the two fragments takes place through the binding of the platinum to the alkyne in an η^2 fashion and additional support may be provided through a Pt–Pt interaction. Binuclear complexes showing similar kinds of interactions have been reported previously.[22] Through this interaction, the COD-free platinum(II) fragment acting as a fifth ligand on the *cis* platinum complex **5a** could then undergo pseudorotation followed by expulsion, resulting in the formation of the *trans* complex. The fact that only *trans* **4b** and no *trans* **5b** was obtained corroborates the participation of the [Pt(cod)(C≡CC_6H_5)$_2$] precursor in the conversion of the *cis* to the *trans* isomer. Although we were able to obtain the desired *trans* compound by treating the *cis* isomer with the precursor, the thermally induced isomerization reaction was pursued with a view to obtaining the *trans* compound in good yield.

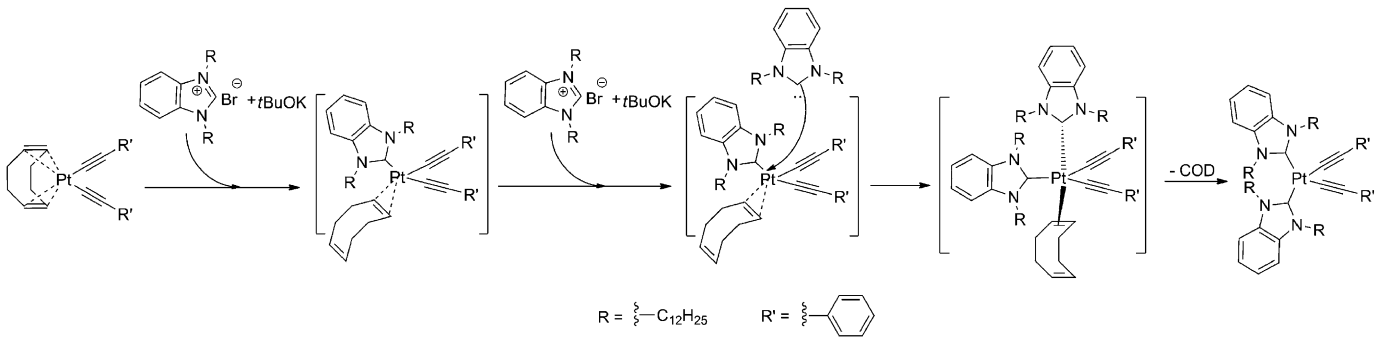

Scheme 2. Proposed reaction path for the formation of *cis* complex **5a**.

Thermally induced isomerization: In order to test the propensity of our complexes to undergo thermally induced isomerization,[39e,44] thermogravimetric analysis (TGA) and differential scanning calorimetry (DSC) measurements were carried out on complexes **5a** and **5b** (Figures S14–S16 in the Supporting Information). The data from these measurements revealed the isomerization to progress at high temperatures around 200 °C and, based on these experiments, we were also able to obtain an isomerization enthalpy ΔH_{isom} of $-4.5\ kcal\,mol^{-1}$ by using $RbNO_3$ as a calibration standard (Figure S17 in the Supporting Information). This value is in good accordance with the relative thermodynamic stability of the *trans* isomer **5b** over the *cis* isomer **5a**, estimated as $-6.0\ kcal\,mol^{-1}$ by DFT calculations (see the Supporting Information).

The results from the DSC studies were further verified by heating the neat complex **5a** in a J. Young NMR tube at 200 °C for 6 h under an inert atmosphere. The black-brown residue obtained after the reaction was chromatographed on silica gel to obtain a colorless product, which was confirmed as the *trans* complex **5b** based on ^1H NMR studies. The yield of **5b** was found to be 64 %. Investigation of one of the fractions collected during chromatography showed it to contain a trace amount of diphenylbutadiyne (confirmed on the basis of GC-MS analysis). Although one could attribute the formation of this molecule to reductive elimination from the *cis* complex, it still does not entirely clarify the conversion process. Previous mechanistic studies on platinum complexes bearing phosphine or pyridine ligands have suggested that *cis–trans* isomerization either proceeds by a dissociative mechanism that involves loss of the phosphine, pyridine, or halide ligands leading to a three-coordinate T-shaped complex intermediate, or by an associative mechanism that involves coordination of the phosphine or pyridine ligand leading to a five-coordinate intermediate.[45] We found that the conversion of complex **5a** to **5b** proceeded efficiently when **5a** was heated in [D_8]toluene at 200 °C for 2 days in a J. Young NMR tube to give an isolated yield of 73 %. The reaction was found to proceed more slowly than that carried out in the neat solid. Performing the reaction in the presence of the free carbene ligand and *t*BuOK neither accelerated nor retarded formation of the product.

Furthermore, when complex **5a** was heated in the presence of the carbene ligand IBIM and *t*BuOK, no incorporation of IBIM in the final *trans* product was found. This observation disfavors dissociation of the carbene ligand during the isomerization process and is consistent with the theoretical study since the calculated carbene dissociation enthalpy was as high as $54.6\ kcal\,mol^{-1}$ (see the Supporting Information). Considering the temperature at which the reaction was performed, such dissociation can be ruled out. The observation of a small amount of diphenylbutadiyne, as mentioned above, may be attributed to reductive elimination of the alkyne ligands from the *cis* complex. This would generate the corresponding biscarbene Pt^0 complex, which is isolobal with a carbene ligand. The in situ generated small amount of Pt^0 complex could then associate with a molecule of the four-coordinate *cis* complex to form a pentacoordinate complex stabilized through a Pt^0–Pt^{II} interaction. This could then undergo pseudorotation, resulting in expulsion of the Pt^0 complex and leading to formation of the desired *trans* Pt^{II} complex. Acting like a catalyst, the Pt^0 complex could coordinate to another *cis* complex and could repeat the same process over and over again to transform all of the *cis* complex into the corresponding *trans* complex. In this way, the Pt^0 complex would only be required in catalytic amounts, which would be consistent with the small amount of diphenylbutadiyne expelled during the entire reaction and the obtained high yield of the *trans* complex. The need for such elevated temperatures for the isomerization to proceed is further corroborated by the DFT-calculated energy of activation of $34.9\ kcal\,mol^{-1}$ (see the optimized transition state in the Supporting Information) required for reductive elimination of the alkyne ligands. It is important to note that, although rare, well-defined Pt^0 species bearing carbene ligands have recently been isolated and characterized by Braunschweig and co-workers.[46] In order to further confirm our hypothesis, we performed a scrambling experiment between two *cis* complexes bearing different carbene ligands. To this end, we synthesized complex **9a** bearing the IBIM ligand instead of the DBIM ligand as in the case of complex **5a**. For comparison, complex **9b** was also synthesized and characterized separately. A 1:1 mixture of **5a** and **9a** in toluene was heated at 200 °C for 2 days, and subsequent workup gave complexes **5b** and **9b** as the major products. We were also able to isolate and characterize the new complex **10**, in which both IBIM and DBIM are ligated to the Pt^{II} center. The structure of **10** was confirmed by various NMR and MS studies. The formation of **10** is supportive of scrambling of the NHC ligand during the *cis* to *trans* conversion, although our earlier experiments suggested no dissociation of the free carbene ligand. We presume that transfer of the ligand proceeds through bridging of the carbene ligand between the two platinum centers, which could well facilitate the scrambling without the need for complete dissociation of the carbene ligand. Based on the above experimental observations, a preliminary mechanism is proposed in Scheme 3.

Conclusion

We have presented the synthesis and characterization of a new class of triplet emitter molecules based on NHC-ligated platinum(II) acetylide complexes. A viable synthetic route for a series of *cis* and *trans* complexes of the type [Pt(dbim)$_2$(C≡CR)$_2$] is reported. Although the yields of *trans* isomers obtained by a direct approach were very low, we have demonstrated that they can be significantly improved by employing different reaction conditions starting from the readily available *cis* NHC Pt^{II} acetylide complexes. Experimental and theoretical studies of the photophysical properties of the complexes have revealed very interesting luminescent properties, with two of the complexes displaying the

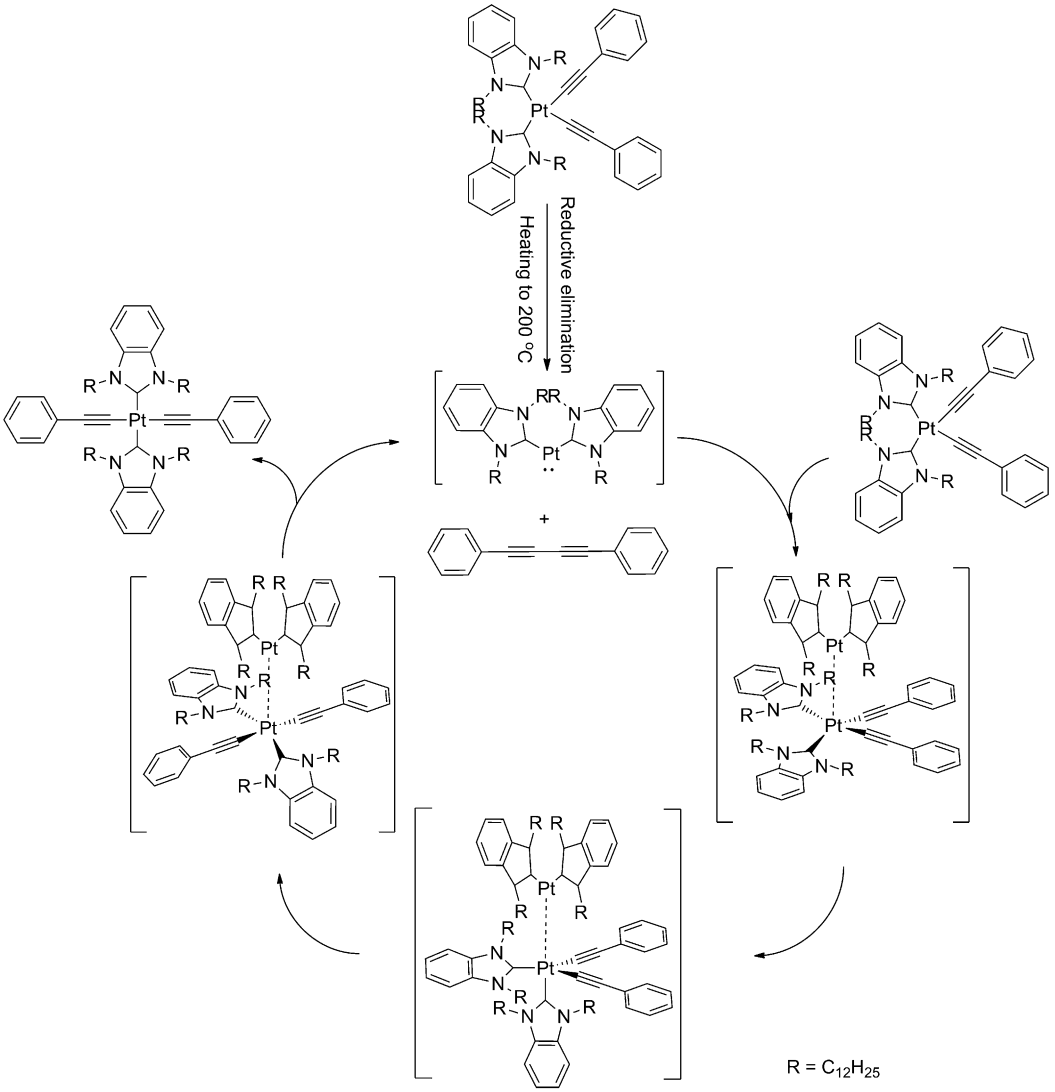

Scheme 3. Proposed isomerization path from **5a** to **5b**.

highest quantum yields hitherto reported for deep-blue emitters in the solid state. The properties of the NHC-bearing Pt^{II} acetylide complexes are very different to those of the non-emissive complex $[Pt(PBu_3)_2(C{\equiv}CC_6H_5)_2]$ and the mostly green-emitting $[Pt(diimine)_2(C{\equiv}CC_6H_5)_2]$ complexes. Experimental results coupled with DFT and TD-DFT calculations have indicated that the emission is intrinsically a mixture of metal-perturbed ^{3}IL with a small contribution from ^{3}MLCT. Close examination of the synthetic reaction revealed the *cis* complexes to be the kinetically favored isomers and the *trans* complexes to be the more thermodynamically stable isomers. Detailed investigations have been carried out with a view to improving the yield of the *trans* products. The *cis* to *trans* isomerization was found to be strongly influenced by temperature, light, and the precursor complex $[Pt(cod)(C{\equiv}CR)_2]$. Based on preliminary mechanistic studies, a solvent-stabilized Pt^{II} dialkyne complex and a bis-NHC Pt^0 species serving as a catalyst are invoked as being involved in the key transformation of the *cis* to the *trans* isomer. DSC measurements have further confirmed the *trans* isomer as the thermodynamically stable product and the isomerization enthalpy (ΔH_{isom}) was found to be 4.5 kcal mol^{-1}. The novel structural and electronic features of the presented complexes, coupled with their interesting luminescent properties in solution, at 10 wt% in PMMA films, and in the solid state, opens up new opportunities for studying a wide range of optical and electronic (or electrochemical) properties.

Acknowledgements

The authors wish to thank Prof. Heinz Berke for scientific discussions, Dr. Thomas Fox for help with NMR studies, and Dr. Ferdinand Wild for DSC and TGA measurements. Financial support from the Swiss National Science Foundation (Grant no. 200021-135488) and the University of Zürich is gratefully acknowledged.

[1] a) M. E. Thompson, *MRS Bull.* **2007**, *32*, 694; b) W.-Y. Wong, P. D. Parvey, *Macromol. Rapid Commun.* **2010**, *31*, 671; c) H. Yersin, A. F. Rausch, R. Czerwieniec, T. Hofbeck, T. Fischer, *Coord. Chem. Rev.* **2011**, *255*, 2622; d) Y. Unger, D. Meyer, O. Molt, C. Schildknecht, I. Münster, G. Wagenblast, T. Strassner, *Angew. Chem.* **2010**, *122*, 10412; *Angew. Chem. Int. Ed.* **2010**, *49*, 10214; e) K. Li, G. Cheng, C. Ma, X. Guan, W.-M. Kwok, Y. Chen, W. Lu, C.-M. Che, *Chem. Sci.* **2013**, *4*, 2630; f) Z. M. Hudson, C. Sun, M. G. Helander, Y.-L. Chang, Z.-H. Lu, S. Wang, *J. Am. Chem. Soc.* **2012**, *134*, 13930; g) H.-F. Xiang, S.-W. Lai, P. T. Lai, C.-M. Che in *Highly Efficient OLEDs with Phosphorescent Materials* (Ed.: H. Yersin), Wiley-VCH, Weinheim, **2008**, pp. 259; h) J. A. G. Williams, *Topics in Current Chemistry, Vol. 281, Photochemistry and Photophysics of Coordination Compounds: Platinum*, Springer, Heidelberg, **2007**; i) Y. Chi, P.-T. Chou, *Chem. Soc. Rev.* **2010**, *39*, 638; j) S.-Y. Chang, J.-L. Chen, Y. Chi, Y.-M. Cheng, G.-H. Lee, C.-M. Jiang, P.-T. Chou, *Inorg. Chem.* **2007**, *46*, 11202; k) H. Yersin, W. Finkenzeller in *Highly Efficient OLEDs with Phosphorescent Materials* (Ed.: H. Yersin), Wiley-VCH, Weinheim, **2008**, p. 15.

[2] a) S. W. Thomas, K. Venkatesan, P. Müller, T. M. Swager, *J. Am. Chem. Soc.* **2006**, *128*, 16641; b) Z. M. Hudson, C. Sun, K. J. Harris, B. E. G. Lucier, R. W. Schurko, S. Wang, *Inorg. Chem.* **2011**, *50*, 3447; c) C.-S. Lee, R. R. Zhuang, S. Sabiah, J.-C. Wang, W.-S. Hwang, I. J. B. Lin, *Organometallics* **2011**, *30*, 3897; d) Q.-Z. Yang, L.-Z. Wu, H. Zhang, B. Chen, Z.-X. Wu, L.-P. Zhang, C.-H. Tung, *Inorg. Chem.* **2004**, *43*, 5195; e) L.-Y. Zhang, L.-J. Xu, X. Zhang, J.-Y. Wang, J. Li, Z.-N. Chen, *Inorg. Chem.* **2013**, *52*, 5167.

[3] a) R. Zieba, C. Desroches, F. Chaput, M. Carlsson, B. Eliasson, C. Lopes, M. Lindgren, S. Parola, *Adv. Funct. Mater.* **2009**, *19*, 235; b) C. K. M. Chan, C.-H. Tao, H.-L. Tam, N. Zhu, V. W.-W. Yam, K.-W. Cheah, *Inorg. Chem.* **2009**, *48*, 2855; c) C. K. M. Chan, C.-H. Tao, K.-F. Li, K. M.-C. Wong, N. Zhu, K.-W. Cheah, V. W.-W. Yam, *Dalton Trans.* **2011**, *40*, 10670; d) R. Liu, A. Azenkeng, D. Zhou, Y. Li, K. D. Glusac, W. Sun, *J. Phys. Chem. A* **2013**, *117*, 1907.

[4] a) P. Du, J. Schneider, P. Jarosz, R. Eisenberg, *J. Am. Chem. Soc.* **2006**, *128*, 7726; b) X. Wang, S. B. Goeb, Z. Ji, N. A. Pogulaichenko, F. N. Castellano, *Inorg. Chem.* **2011**, *50*, 705; c) M. N. Roberts, J. K. Nagle, M. B. Majewski, J. G. Finden, N. R. Branda, M. O. Wolf, *Inorg. Chem.* **2011**, *50*, 4956.

[5] a) G.-J. Zhou, W.-Y. Wong, *Chem. Soc. Rev.* **2011**, *40*, 2541; b) F. Guo, W. Sun, Y. Liu, K. Schanze, *Inorg. Chem.* **2005**, *44*, 4055.

[6] a) M. J. Currie, J. K. Mapel, T. D. Heidel, S. Goffri, M. A. Baldo, *Science* **2008**, *321*, 226; b) W. Wu, J. Zhang, H. Yang, B. Jin, Y. Hu, J. Hua, C. Jing, Y. Long, H. Tian, *J. Mater. Chem.* **2012**, *22*, 5382; c) W.-Y. Wong, C.-L. Ho, *Acc. Chem. Res.* **2010**, *43*, 1246.

[7] M. Montalti, A. Credi, L. Prodi, M. T. Gandolfi, *Handbook of Photochemistry*, 3rd ed., Taylor & Francis Group, Boca Raton, **2006**.

[8] a) M. L. Muro, A. A. Rachfor, X. Wang, F. N. Castellano in *Topics in Organometallic Chemistry, Vol. 29, Photophysics of Organometallics* (Ed.: A. J. Lees), Springer Verlag, Berlin, **2010**, p. 159; b) V. W.-W. Yam, *Acc. Chem. Res.* **2002**, *35*, 555; c) T. Sajoto, P. I. Djurovich, A. Tamayo, M. Yousufuddin, R. Bau, M. E. Thompson, R. J. Holmes, S. R. Forrest, *Inorg. Chem.* **2005**, *44*, 7992.

[9] J. Chatt, B. L. Shaw, *J. Chem. Soc.* **1959**, 4020.

[10] a) M. N. Roberts, C.-J. Carling, J. K. Nagle, N. R. Branda, M. O. Wolf, *J. Am. Chem. Soc.* **2009**, *131*, 16644; b) G. Ramakrishna, T. Goodson, J. E. Rogers-Haley, T. M. Cooper, D. G. McLean, A. Urbas, *J. Phys. Chem. C* **2009**, *113*, 1060; c) K. Haskins-Glusac, I. Ghiviriga, K. A. Abboud, K. S. Schanze, *J. Phys. Chem. B* **2004**, *108*, 4969.

[11] a) K. Glusac, M. E. Köse, H. Jiang, K. S. Schanze, *J. Phys. Chem. B* **2007**, *111*, 929; b) T. Cardolaccia, Y. Li, K. S. Schanze, *J. Am. Chem. Soc.* **2008**, *130*, 2535; c) J. Stahl, J. C. Bohling, T. B. Peters, L. D. Quadras, J. A. Gladysz, *Pure Appl. Chem.* **2008**, *80*, 459; d) Q. Zheng, J. C. Bohling, T. B. Peters, A. C. Frisch, F. Hampel, J. A. Gladysz, *Chem. Eur. J.* **2006**, *12*, 6486; e) Y. Liu, S. Jiang, K. Glusac, D. H. Powell, D. F. Anderson, K. S. Schanze, *J. Am. Chem. Soc.* **2002**, *124*, 12412.

[12] C.-H. Tao, N. Zhu, V. W.-W. Yam, *Chem. Eur. J.* **2005**, *11*, 1647.

[13] a) W.-Y. Wong, C.-K. Wong, G.-L. Lu, A. W.-M. Lee, K.-W. Cheah, J.-X. Shi, *Macromolecules* **2003**, *36*, 983; b) K. Sonogashira, S. Takahashi, N. Hagihara, *Macromolecules* **1977**, *10*, 879; c) K. A. Williams, A. J. Boydston, C. W. Bielawski, *Chem. Soc. Rev.* **2007**, *36*, 729.

[14] C.-W. Chan, L.-K. Cheng, C.-M. Che, *Coord. Chem. Rev.* **1994**, *132*, 87.

[15] a) M. Hissler, W. B. Connick, D. K. Geiger, J. E. McGarrah, D. Lipa, R. J. Lachicotte, R. Eisenberg, *Inorg. Chem.* **2000**, *39*, 447; b) J. E. McGarrah, R. Eisenberg, *Inorg. Chem.* **2003**, *42*, 4355; c) T. J. Wadas, S. Chakraborty, R. J. Lachicotte, Q.-M. Wang, R. Eisenberg, *Inorg. Chem.* **2005**, *44*, 2628; d) J. Schneider, P. Du, P. Jarosz, T. Lazarides, X. Wang, W. W. Brennessel, R. Eisenberg, *Inorg. Chem.* **2009**, *48*, 4306; e) P. Jarosz, K. Lotito, J. Schneider, D. Kumaresan, R. Schmehl, R. Eisenberg, *Inorg. Chem.* **2009**, *48*, 2420; f) M. Hissler, J. E. McGarrah, W. B. Connick, D. K. Geiger, S. D. Cummings, R. Eisenberg, *Coord. Chem. Rev.* **2000**, *208*, 115.

[16] C. E. Whittle, J. A. Weinstein, M. W. George, K. S. Schanze, *Inorg. Chem.* **2001**, *40*, 4053.

[17] a) I. E. Pomestchenko, C. R. Luman, M. Hissler, R. Ziessel, F. N. Castellano, *Inorg. Chem.* **2003**, *42*, 1394; b) F. Hua, S. Kinayyigit, J. R. Cable, F. N. Castellano, *Inorg. Chem.* **2005**, *44*, 471; c) F. Hua, S. Kinayyigit, J. R. Cable, F. N. Castellano, *Inorg. Chem.* **2006**, *45*, 4304.

[18] a) W.-S. Tang, X.-X. Lu, K. M.-C. Wong, V. W.-W. Yam, *J. Mater. Chem.* **2005**, *15*, 2714; b) A. Y.-Y. Tam, W. H. Lam, K. M.-C. Wong, N. Zhu, V. W.-W. Yam, *Chem. Eur. J.* **2008**, *14*, 4562.

[19] a) V. W.-W. Yam, K. M.-C. Wong, N. Zhu, *J. Am. Chem. Soc.* **2002**, *124*, 6506; b) S. C. F. Kui, Y.-C. Law, G. S. M. Tong, W. Lu, M.-Y. Yuen, C.-M. Che, *Chem. Sci.* **2011**, *2*, 221; c) Q.-Z. Yang, L.-Z. Wu, Z.-X. Wu, L.-P. Zhang, C.-H. Tung, *Inorg. Chem.* **2002**, *41*, 5653; d) R. McGuire, Jr., M. C. McGuire, D. R. McMillin, *Coord. Chem. Rev.* **2010**, *254*, 2574; e) X. Han, L.-Z. Wu, G. Si, J. Pan, Q.-Z. Yang, L.-P. Zhang, C.-H. Tung, *Chem. Eur. J.* **2007**, *13*, 1231; f) H.-M. Wen, Y.-H. Wu, Y. Fan, L.-Y. Zhang, C.-N. Chen, Z.-N. Chen, *Inorg. Chem.* **2010**, *49*, 2210.

[20] a) R. Liu, Y. Li, Y. Li, H. Zhu, W. Sun, *J. Phys. Chem. A* **2010**, *114*, 12639; b) W. Lu, B.-X. Mi, M. C. W. Chan, Z. Hui, C.-M. Che, N. Zhu, S.-T. Lee, *J. Am. Chem. Soc.* **2004**, *126*, 4958; c) Z. Wang, E. Turner, V. Mahoney, S. Madakuni, T. Groy, J. Li, *Inorg. Chem.* **2010**, *49*, 11276; d) D. L. Rochester, S. Develay, S. Zalis, J. A. G. Williams, *Dalton Trans.* **2009**, 1728; e) P. Shao, Y. Li, A. Azenkeng, M. R. Hoffmann, W. Sun, *Inorg. Chem.* **2009**, *48*, 2407.

[21] S.-C. Chan, M. C. W. Chan, Y. Wang, C.-M. Che, K.-K. Cheung, N. Zhu, *Chem. Eur. J.* **2001**, *7*, 4180.

[22] S. Fernández, J. Fornies, B. Gil, J. Gomez, E. Lalinde, *Dalton Trans.* **2003**, 822.

[23] a) G. C. Vougioukalakis, R. H. Grubbs, *Chem. Rev.* **2010**, *110*, 1746; b) W. A. Herrmann, C. Köcher, *Angew. Chem.* **1997**, *109*, 2256; *Angew. Chem. Int. Ed. Engl.* **1997**, *36*, 2162; c) T. Fleetham, Z. Wang, J. Li, *Org. Electron.* **2012**, *13*, 1430.

[24] D. Bourissou, O. Guerret, F. P. Gabbaï, G. Bertrand, *Chem. Rev.* **2000**, *100*, 39.

[25] A. J. Boydston, K. A. Williams, C. W. Bielawski, *J. Am. Chem. Soc.* **2005**, *127*, 12496.

[26] a) Y. Unger, A. Zeller, S. Ahrens, T. Strassner, *Chem. Commun.* **2008**, 3263; b) Y. Unger, A. Zeller, M. A. Taige, T. Strassner, *Dalton Trans.* **2009**, 4786; c) Y. Unger, D. Meyer, T. Strassner, *Dalton Trans.* **2010**, *39*, 4295.

[27] M. Koch, J. A. Garg, O. Blacque, K. Venkatesan, *J. Organomet. Chem.* **2012**, *700*, 154.

[28] Y. Zhang, J. A. Garg, C. Michelin, T. Fox, O. Blacque, K. Venkatesan, *Inorg. Chem.* **2011**, *50*, 1220.

[29] Y. Han, H. V. Huynh, G. K. Tan, *Organometallics* **2007**, *26*, 4612.

[30] a) M. Herberhold, T. Schmalz, W. Milius, B. Wrackmeyer, *J. Organomet. Chem.* **2002**, *641*, 173; b) A. García, E. Lalinde, M. T. Moreno, *Eur. J. Inorg. Chem.* **2007**, 3553.

[31] Q.-X. Liu, F.-B. Xu, Q.-S. Li, H.-B. Song, Z.-Z. Zhang, *J. Mol. Struct.* **2004**, *697*, 131.

[32] S. D. Adhikary, D. Bose, P. Mitra, K. D. Saha, V. Bertolasi, J. Dinda, *New J. Chem.* **2012**, *36*, 759.
[33] M. S. Khan, R. K. M. Al-Saadi, L. Male, P. R. Raithby, J. K. Bjernemose, *Acta Crystallogr. Sect. E* **2003**, *59*, m774.
[34] Gaussian 03, Revision D.01, M. J. Frisch, G. W. Trucks, H. B. Schlegel, G. E. Scuseria, M. A. Robb, J. R. Cheeseman, J. A. Montgomery, Jr., T. Vreven, K. N. Kudin, J. C. Burant, J. M. Millam, S. S. Iyengar, J. Tomasi, V. Barone, B. Mennucci, M. Cossi, G. Scalmani, N. Rega, G. A. Petersson, H. Nakatsuji, M. Hada, M. Ehara, K. Toyota, R. Fukuda, J. Hasegawa, M. Ishida, T. Nakajima, Y. Honda, O. Kitao, H. Nakai, M. Klene, X. Li, J. E. Knox, H. P. Hratchian, J. B. Cross, V. Bakken, C. Adamo, J. Jaramillo, R. Gomperts, R. E. Stratmann, O. Yazyev, A. J. Austin, R. Cammi, C. Pomelli, J. W. Ochterski, P. Y. Ayala, K. Morokuma, G. A. Voth, P. Salvador, J. J. Dannenberg, V. G. Zakrzewski, S. Dapprich, A. D. Daniels, M. C. Strain, O. Farkas, D. K. Malick, A. D. Rabuck, K. Raghavachari, J. B. Foresman, J. V. Ortiz, Q. Cui, A. G. Baboul, S. Clifford, J. Cioslowski, B. B. Stefanov, G. Liu, A. Liashenko, P. Piskorz, I. Komaromi, R. L. Martin, D. J. Fox, T. Keith, M. A. Al-Laham, C. Y. Peng, A. Nanayakkara, M. Challacombe, P. M. W. Gill, B. Johnson, W. Chen, M. W. Wong, C. Gonzalez, J. A. Pople, Gaussian, Inc., Wallingford CT, **2004**.
[35] C. Adamo, V. Barone, *J. Chem. Phys.* **1999**, *110*, 6158.
[36] T. H. Dunning, P. J. Hay in *Modern Theoretical Chemistry, Vol. 3* (Ed.: H. F. Schaefer), Plenum, New York, **1976**.
[37] R. Ditchfield, W. J. Hehre, J. A. Pople, *J. Chem. Phys.* **1971**, *54*, 724.
[38] a) J. Chatt, R. G. Wilkins, *J. Chem. Soc.* **1952**, 273; b) J. Chatt, R. G. Wilkins, *J. Chem. Soc.* **1952**, 4300.
[39] a) D. T. Rosevear, F. G. A. Stone, *J. Chem. Soc.* **1965**, 5275; b) D. A. Redfield, J. H. Nelson, *J. Am. Chem. Soc.* **1974**, *96*, 6219; c) W. J. Louw, *Inorg. Chem.* **1977**, *16*, 2147; d) R. Romeo, M. R. Plutino, L. I. Elding, *Inorg. Chem.* **1997**, *36*, 5909; e) J. H. Price, J. P. Birk, B. B. Wayland, *Inorg. Chem.* **1978**, *17*, 2245; f) J. Burgess, M. E. Howden, R. D. W. Kemmitt, N. S. Sridhara, *J. Chem. Soc. Dalton Trans.* **1978**, 1577; g) J. Vicente, A. Arcas, M.-D. Galvez-Lopez, P. G. Jones, *Organometallics* **2006**, *25*, 4247.
[40] G. K. Anderson, R. J. Cross, *Chem. Soc. Rev.* **1980**, *9*, 185, and references therein.
[41] N. Oberbeckmann, K. Merz, R. A. Fischer, *Organometallics* **2001**, *20*, 3265.
[42] The reactions of *cis* isomer **5a** with different combinations were probed by ^{1}H NMR studies involving: 1) THF, 2) [dbimH]Br, 3) [dbimH]Br and *t*BuOK, 4) KBr, 5) *t*BuOK, 6) *t*BuOH, and 7) cyclooctadiene (COD). No isomerization was detected.
[43] a) R. J. Puddephatt, P. J. Thompson, *J. Chem. Soc. Dalton Trans.* **1977**, 1219; b) C. Eaborn, K. J. Odell, A. Pidcock, *J. Chem. Soc. Dalton Trans.* **1978**, 1288.
[44] a) P. Haake, T. A. Hylton, *J. Am. Chem. Soc.* **1962**, *84*, 3774; b) R. Ellis, T. A. Weil, M. Orchin, *J. Am. Chem. Soc.* **1970**, *92*, 1078; c) J. R. Perumareddi, A. W. Adamson, *J. Phys. Chem.* **1968**, *72*, 414; d) B. Cetinkaya, E. Cetinkaya, M. F. Lappert, *J. Chem. Soc. Dalton Trans.* **1973**, 906.
[45] a) F. Yamashita, H. Kuniyasu, J. Terao, N. Kambe, *Inorg. Chem.* **2006**, *45*, 1399; b) W. Baratta, S. Stoccoro, A. Doppiu, E. Herdtweck, A. Zucca, P. Rigo, *Angew. Chem.* **2003**, *115*, 109; *Angew. Chem. Int. Ed.* **2003**, *42*, 105; c) E. Guido, G. D'Amico, N. Russo, E. Sicilia, S. Rizzato, A. Albinati, A. Romeo, M. R. Plutino, R. Romeo, *Inorg. Chem.* **2011**, *50*, 2224; d) S. Fantasia, H. Jacobsen, L. Cavallo, S. P. Nolan, *Organometallics* **2007**, *26*, 3286.
[46] J. Bauer, H. Braunschweig, P. Brenner, K. Kraft, K. Radacki, K. Schwab, *Chem. Eur. J.* **2010**, *16*, 11985.

Received: June 10, 2013
Revised: July 25, 2013
Published online: September 25, 2013

